

Investigating the efficiency of the Beijing Faint Object Spectrograph and Camera (BFOSC) of the Xinglong 2.16-m reflector

Yong Zhao^{1,2}, Zhou Fan¹, Juan-Juan Ren¹, Liang Ge¹, Xiao-Ming Zhang¹, Hong-Bin Li¹,
Hui-Juan Wang¹, Jian-Feng Wang¹, Peng Qiu^{1,2} and Xiao-Jun Jiang^{1,3}

¹ Key Laboratory of Optical Astronomy, National Astronomical Observatories, Chinese Academy of Sciences, Beijing 100101, China; zhaoyong@nao.cas.cn

² University of Chinese Academy of Sciences, Beijing 100049, China

³ School of Astronomy and Space Science, University of Chinese Academy of Sciences, Beijing 100049, China

Received 2018 January 20; accepted 2018 April 26

Abstract The Beijing Faint Object Spectrograph and Camera (BFOSC) is one of the most important instruments operating in conjunction with the 2.16-m telescope at Xinglong Observatory. Every year there are ~ 20 SCI-papers published based on observational data acquired with this telescope. In this work, we have systemically measured the total efficiency of the BFOSC that operates as part of the 2.16-m reflector, based on observations of two ESO flux standard stars. We have obtained the total efficiencies of the BFOSC instrument of different grisms with various slit widths in almost all ranges, and analyzed factors which effect the efficiency of this telescope and spectrograph. For astronomical observers, the result will be useful for them to select a suitable slit width, depending on their scientific goals and weather conditions during observations. For technicians, the result will help them to systemically identify the real efficiency of the telescope and spectrograph, and to further improve the total efficiency and observing capacity of the telescope technically.

Key words: astronomical instrumentation, methods and techniques — instrumentation: spectrographs

1 INTRODUCTION

The Xinglong 2.16-m reflector is an English equatorial mount telescope at Xinglong Observatory (XO), with an effective aperture of 2.16 meters, and a focal ratio of $f/9$ at the Cassegrain focus (Su et al. 1989). It is the first 2-meter class astronomical telescope in China. The 2.16-m reflector is equipped with three main instruments currently: (1) the Beijing Faint Object Spectrograph and Camera (BFOSC), which is used for intermediate and low-resolution ($R \sim 500 - 2000$) spectroscopy; (2) the OMR spectrograph (an instrument made by Optomechanics Research Inc., based in Tucson, Arizona), which is used for low resolution spectroscopy, with similar spectral resolutions as the BFOSC; (3) the High Resolution Spectrograph (HRS), which is used for

fiber-fed high-resolution ($R \sim 30\,000 - 65\,000$) spectroscopy. A detailed introduction for these three instruments that are used in conjunction with the Xinglong 2.16-m reflector can be found in Fan et al. (2016).

Many telescopes and spectrographs around the world have efficiency estimations which are listed on their websites. For example, the system efficiency of the High Efficiency and Resolution Multi-Element Spectrograph (HERMES) at the 3.9-m Anglo-Australian Telescope (Wampler & Morton 1977) is from 6% to 8% and is used for Galactic Archaeology ($V = 14$). This estimation includes the efficiency of telescope, fiber system, spectrograph, and detector (Sheinis et al. 2015). The system efficiencies of the High Resolution Echelle Spectrograph of the Lijiang 2.4-m telescope, administered by Yunnan Observatories, are 2% for fiber diameter

of 1.2'' and 3% for fiber diameter of 2.0''¹. The European Southern Observatory (ESO) Faint Object Spectrograph and Camera (EFOSC) that is part of the ESO 3.6-m telescope has different grisms², most of which have system efficiencies around 30%. However, for all the telescopes mentioned above, the efficiencies of spectrographs with different slits and different grisms have not been measured systemically and detailedly. According to statistics compiled during the recent 10 years, the most frequently used instrument (almost up to half of the 2.16-m reflector's observing time) is the BFOSC.

In this work, we investigate the total efficiency of the telescope on which BFOSC is mounted, and make some suggestions for the telescope users and technicians. This paper is organized as follows:

Section 2 is an introduction to XO; in Section 3.1 and Section 3.2, the observations and data reduction are presented, respectively; in Section 4, we discuss the impacts of slit widths, weather conditions, stellar brightness and mirror reflectivities on the efficiency estimations; finally a brief summary is given in Section 5.

2 THE XINGLONG OBSERVATORY OF NAOC

XO, administered by National Astronomical Observatories, Chinese Academy of Sciences (NAOC), has the coordinates: 40°23' 39''N, 117°34' 30''E, and was founded in 1968. Until now, it is the largest optical astronomical observatory in the Asian continent. There are nine telescopes, with effective aperture greater than 50-cm located at XO. The average altitude of XO is ~960m, and it is located at Xinglong county, Chengde city, Hebei province, which is ~120 km northeast of Beijing. The mean and median seeing values of XO are around 1.9'' and 1.7'', respectively, calculated from over one year of statistics. For most of the time, the mean and median values of wind speed at XO range from 1 m s⁻¹ to 3.5 m s⁻¹, and the sky brightness at zenith is around 21.1 mag arcsec⁻² (*V*-band). About 63% of the nights per year can be used for spectroscopic observations based on the statistics of observational data acquired in 2007 – 2014. A more detailed introduction to the observing conditions at XO can be found in Zhang et al. (2015).

¹ <http://www.gmg.org.cn/v2/detail/instrument/24>

² <http://www.ls.eso.org/sci/facilities/lasilla/instruments/efosc-3p6/docs/Efosc2Grisms.html#grisms>

3 OBSERVATIONS AND DATA REDUCTION

3.1 Observations

In this work, we chose two flux standard stars with different brightnesses from the list of ESO spectrophotometric standard stars³.

Table 1 lists information on the two standard stars, where HD 93521 is ~4 mag brighter than Feige 34 in the *V*-band. Since the efficiency varies greatly with different slit widths and grisms, we can investigate the variation of efficiencies by observing standard stars with different brightnesses. The spectral types of the two standard stars are both O. Therefore, we can eliminate the effects on the efficiency estimations due to the different spectral types of observing targets.

Table 2 presents the parameters of the slits for the BFOSC from Huang et al. (2012). Table 3 lists the parameters of the grisms/prism/echelles for the BFOSC (see Fan et al. 2016 for details). The long slits with a length of 9.4'' in Table 2 are used for spectroscopic observations with the common grisms (No. 2–10 in Table 3), and the short slits are used for spectroscopic observations with the echelles (No. 11–13 in Table 3). Echelle E13 is designed for measuring the velocity field of extended sources with the third order spectrum, and the *V*-band filter is used to remove other orders in the spectrum (Fan et al. 2016).

Table 1 Information on the Two Observed Standard Stars, including the Coordinates, *V* Magnitudes and Spectral Types.

Name	RA	Dec	<i>V</i> (mag)	Spectral type
HD 93521	10:48:23.51	+37:34:12.8	7.04	O
Feige 34	10:39:36.71	+43:06:10.1	11.18	O

Table 2 Parameters of the Slits in BFOSC

Long Slits		Short Slits	
Width	Length	Width	Length
('')	(')	('')	(')
0.6	9.4	0.6	3.5
0.7	9.4	1.0	4.0
1.1	9.4	1.6	3.6
1.4	9.4	2.3	3.7
1.8	9.4	3.2	3.7
2.3	9.4		
3.6	9.4		
7.0	9.4		
14.0	9.4		

³ <http://www.eso.org/sci/observing/tools/standards/spectra.html>

Table 3 Parameters of the Grisms/Prism/Echelles for the BFOSC

Number	Name	Spec.Ord. (m)	Recip. Disp. (Å mm ⁻¹)	Sp. Res. Per Pixel. (Å pix ⁻¹)	Wav. Range (Å)
1	P1		573 – 2547	8.6 – 38.2	4000 – 5600
2	G3	1	139	3.12	3300 – 6600
3	G4	1	198	4.45	3600 – 8700
4	G5	1	199	4.47	5200 – 10 000
5	G6	1	88	1.98	3300 – 5450
6	G7	1	95	2.13	3780 – 6760
7	G8	1	80	1.79	5800 – 8280
8	G10	1	392	8.80	3300 – 10 000
9	G11	1	295	6.63	3600 – 9600
10	G12	1	837	18.8	5200 – 10 000
11	E9+G10	22–10	16.8 – 38.4	0.38 – 0.86	3300 – 10 000
12	E9+G11	18–9	21.0 – 47.9	0.47 – 1.076	3900 – 9800
13	E9+G12	12–6	29.0 – 73.2	0.65 – 1.64	5200 – 10 000
14	E13+V	3	33.1	0.76	4980 – 5990

Table 4 Observation Dates for the Grisms

Date	Grimm
2017–02–19	G3, G4, G5, G6, G7, G8
2017–03–07	G10, G11, G12, E13+V
2017–03–08	E9+G10, E9+G11, E9+G12

For the long slits in BFOSC, most users choose a slit width of 1.8'' or 2.3'', depending on real-time seeing during the observations. While for the short slits of BFOSC, most observers choose slit width of 1.6'' or 2.3''. In this work, we choose the slit widths of 1.8'', 2.3'', 7.0'' and 14.0'' for the long slits; and choose the slit widths of 1.6'' and 2.3'' for the short slits. Our observing strategy is to observe the two standard stars with all the grisms/prism/echelles of the BFOSC with these slit widths. For E13+V, we observe the two standard stars with slit widths of 1.8'', 7.0'' and 14.0''. However, due to limited time, for Feige 34, the slit width of 7.0'' for E13+V and E9+G12 was not observed this time. P1 is a straight prism, which is seldom used, and we do not observe with it.

The spectral quality of all the observations is high, with signal-to-noise ratio (SNR) ≥ 100 . Table 4 presents the observation dates. We observed the two ESO standard stars on 2017 February 19, March 8 and March 9, with the long slits and short slits of BFOSC. The seeing was $\sim 3.0''$ during the observations. For the grisms G4 and G7, we also used the 385LP filter for removing the 2nd-order spectrum with wavelength ≥ 385 nm.

3.2 Data Reduction

The raw data were processed with the standard procedure for data reduction, with commands in Image Reduction and Analysis Facility (IRAF)⁴ and Interactive Data Language (IDL). For the CCD used by BFOSC, the dark current is $<0.002 \text{ e}^- \text{ pixel}^{-1} \text{ s}^{-1}$ (-85°C). We applied the bias and flat-field corrections for object images with the IRAF task *ccdproc*. The IRAF task *dispcor* was used for wavelength calibration, and we obtained the total number of Analog-to-Digital Units (ADUs) in different wavelengths, which is represented as F_{adu} in Equation (1). We downloaded the calibrated spectra of the two standard stars HD 93521 and Feige 34 from the ESO website. Since the wavelength interval from the ESO spectra does not match that of the BFOSC wavelength well, we use the IDL command *interpol* to interpolate the ESO wavelength to our system.

In order to calculate the total efficiency of the system, many factors need to be considered, including the atmospheric extinction, reflectivity of the primary and secondary mirrors, transmissions of grisms and quantum efficiency of the CCD. The total efficiency of the system can be estimated through observing standard stars (see Fan et al. 2016) as follows,

$$\eta(\lambda) = \frac{F_{\text{adu}} \cdot \text{Gain}}{F_{\lambda} \cdot \delta\lambda \cdot S_{\text{tel}}} \quad (1)$$

⁴ IRAF is distributed by the National Optical Astronomy Observatory, which is operated by the Association of Universities for Research in Astronomy, Inc. (AURA) under cooperative agreement with the National Science Foundation.

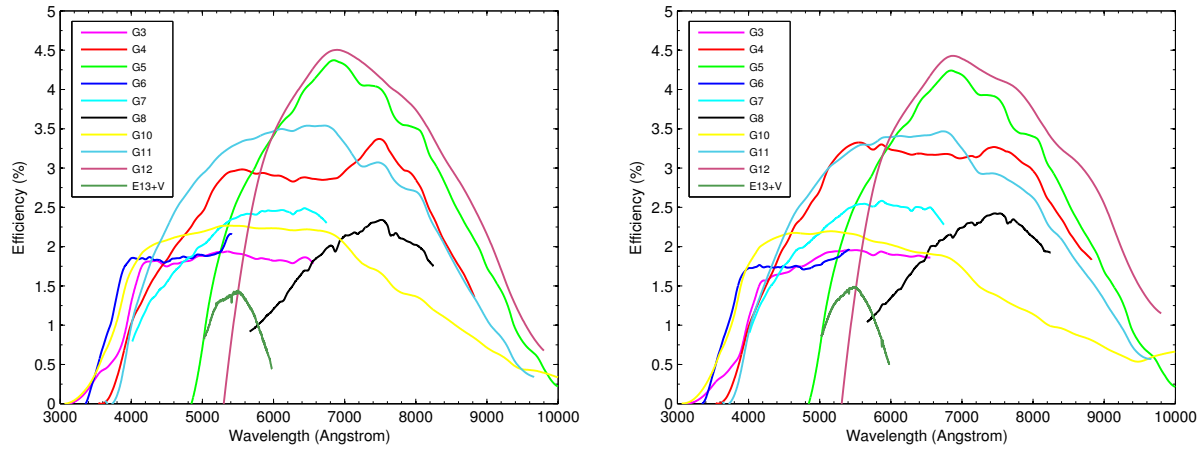


Fig. 1 The total efficiencies of the different gratings used with BFOSC, estimated from observations of Feige 34 (*left panel*) and HD 93521 (*right panel*) with a slit width of $1.8''$. The different colored lines represent different gratings.

where F_{adu} is the observed number counts of a standard star per second (ADU s^{-1}); Gain is the gain of the CCD ($\text{e}^{-1} \text{ADU}^{-1}$); F_{λ} is the theoretical photon flux of a standard star, and we can derive it from its AB mag ($\text{photon s}^{-1} \text{cm}^{-2} \text{\AA}^{-1}$); $\delta\lambda$ is the dispersion of the grating for spectroscopic observations (\AA); S_{tel} is the effective area of the primary mirror of the telescope (cm^2); and λ is the wavelength (\AA).

4 IMPACTS ON THE EFFICIENCY ESTIMATIONS

4.1 Impact of Slit Widths on the Efficiency Estimations

We used Equation (1) to calculate the total efficiency of the telescope with BFOSC, with the different slit widths combined with different gratings/prism/echelles. In fact, there are some absorption lines in the efficiency curves, including the gaseous atmosphere absorption lines (e.g. O_2 , H_2O), the stellar atmosphere absorption lines (e.g. $\text{H}\alpha$, $\text{H}\beta$) and noise. In order to show the efficiency curves more clearly, we smooth all these atmosphere absorption lines.

Figures 1 – 4 show the total efficiencies of Feige 34 and HD 93521 in the wavelengths from $\sim 3000 \text{\AA}$ to $\sim 10000 \text{\AA}$ for the gratings G3/G4/G5/G6/G7/G8/G10/G11/G12/E13+V, with the slit widths of $1.8''$, $2.3''$, $7.0''$, and $14.0''$, respectively. For the slit width of $1.8''$, the peaks of total efficiencies are $\sim 1.7\%$ – 4.5% . For the slit width of $2.3''$, the peaks of total efficiencies are $\sim 2\%$ – 5% . For the slit width of $7.0''$, the

peaks of total efficiencies are $\sim 4.8\%$ – 11% . For the slit width of $14.0''$, the peaks of total efficiencies are $\sim 6.6\%$ – 13% .

Figures 5 and 6 present the results of Feige 34 and HD 93521 at different wavelengths from $\sim 3000 \text{\AA}$ to $\sim 10000 \text{\AA}$ with the slit widths of $1.6''$ and $2.3''$, for E9+G10 and E9+G11, respectively.

Figure 7 displays the results for HD 93521 at different wavelengths from $\sim 5200 \text{\AA}$ to $\sim 10000 \text{\AA}$ with slit widths of $1.6''$ and $2.3''$, for E9+G12. For the slit width of $1.6''$, in Figure 5, the peaks of total efficiencies are $\sim 0.5\%$ – 2.0% , for the wavelengths $\geq 4000 \text{\AA}$; in Figure 6, the peaks of the total efficiencies are $\sim 0.5\%$ – 1.4% , for the wavelengths $\geq 5000 \text{\AA}$; in Figure 7, the peaks of the total efficiencies are $\sim 0.4\%$ – 2.0% , for the wavelengths $\geq 5400 \text{\AA}$. For the slit width of $2.3''$, in Figure 5, the peaks of the total efficiencies are $\sim 1.0\%$ – 3.8% , for the wavelengths $\geq 4000 \text{\AA}$; in Figure 6, the peaks of the total efficiencies are $\sim 0.6\%$ – 1.7% , for the wavelengths $\geq 5000 \text{\AA}$; in Figure 7, the peaks of the total efficiencies are $\sim 0.8\%$ – 5.4% , for the wavelengths $\geq 5400 \text{\AA}$.

4.2 Impact of Stellar Brightness on the Efficiency Estimations

Since the total efficiency estimations may depend on the brightness of the observed stars, we also compare the total efficiencies obtained from the observations of Feige 34 (the fainter one) and HD 93521 (the brighter one).

Figure 8 compares the results of the gratings G3/G4/G5/G6/G7/G8/G10/G11, when observing Feige

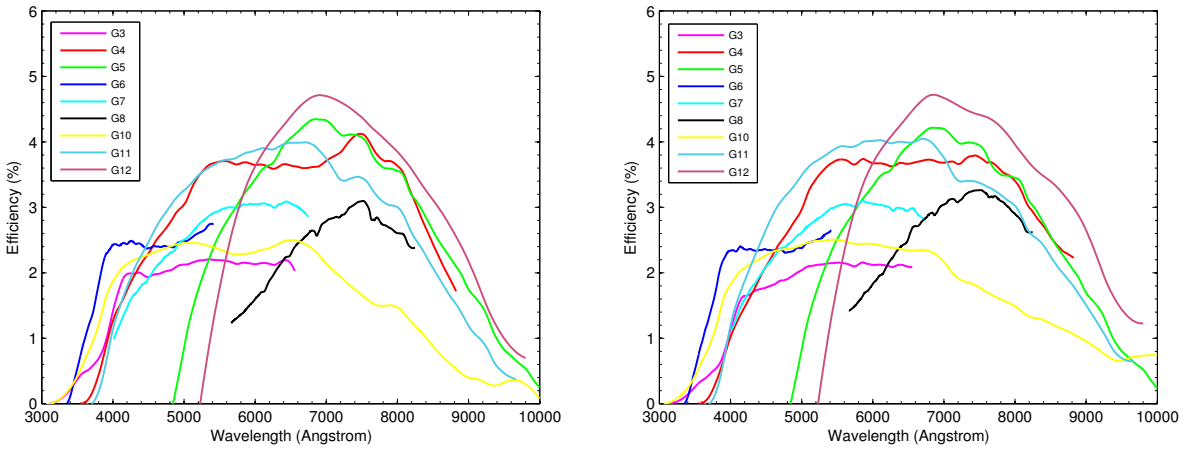


Fig. 2 Same as Fig. 1, but with a slit width of 2.3''.

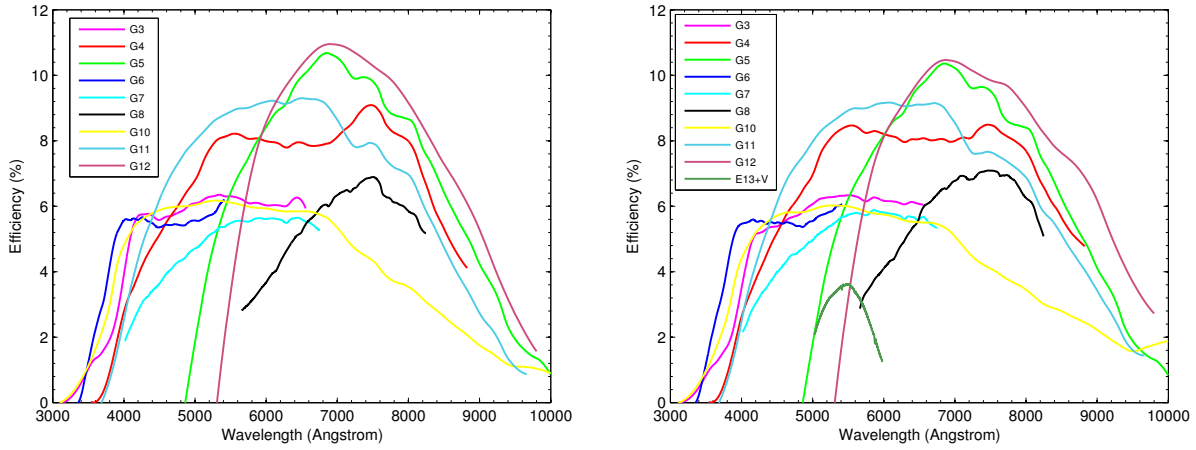


Fig. 3 Same as Fig. 1, but with a slit width of 7.0''.

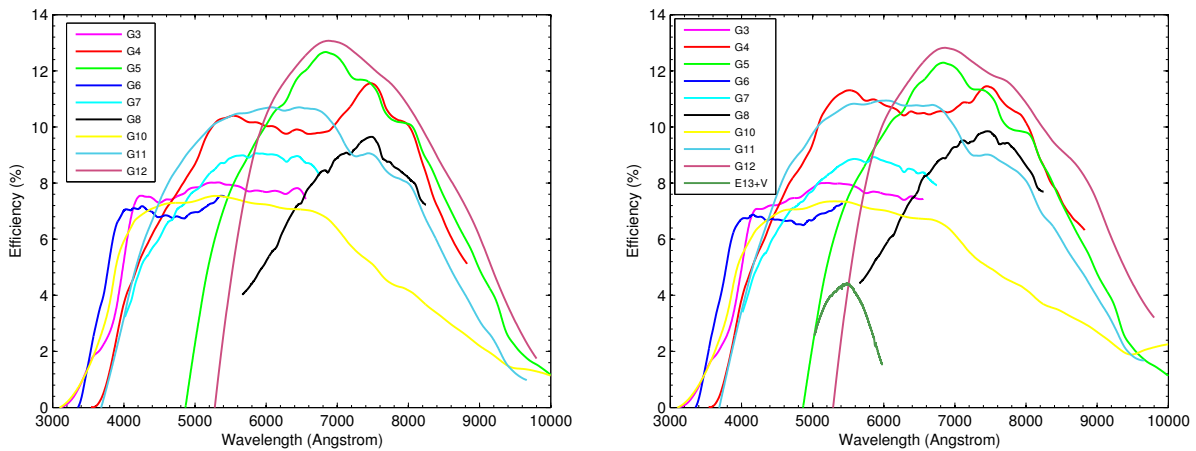


Fig. 4 Same as Fig. 1, but with a slit width of 14.0''.

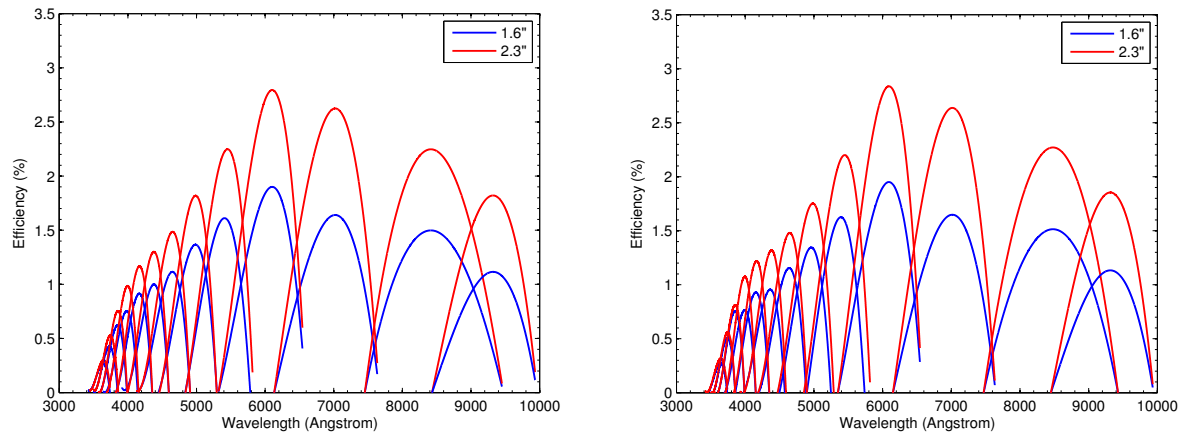


Fig. 5 The total efficiencies of E9+G10, estimated from the observations of Feige 34 (left panel) and HD 93521 (right panel), with slit widths of 1.6'' (blue lines) and 2.3'' (red lines).

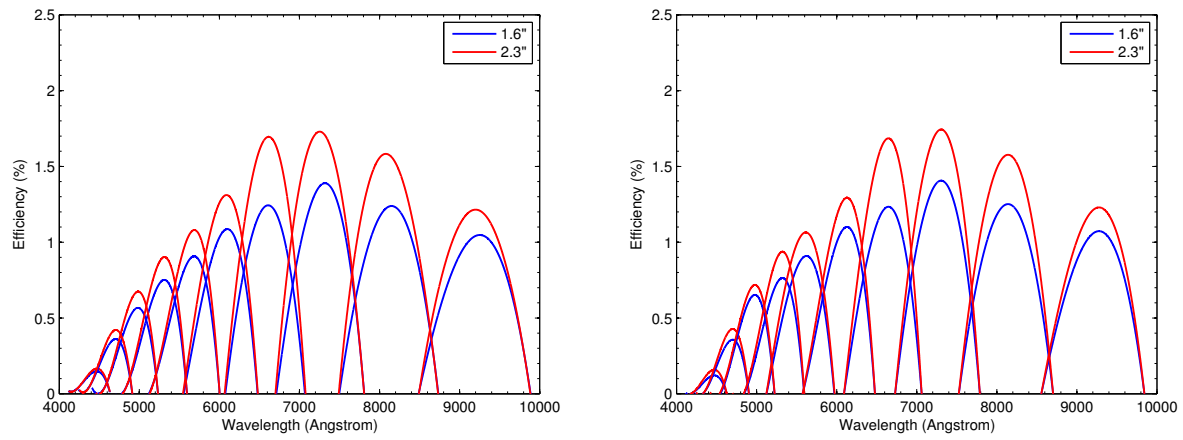


Fig. 6 Same as Fig. 5, but with E9+G11.

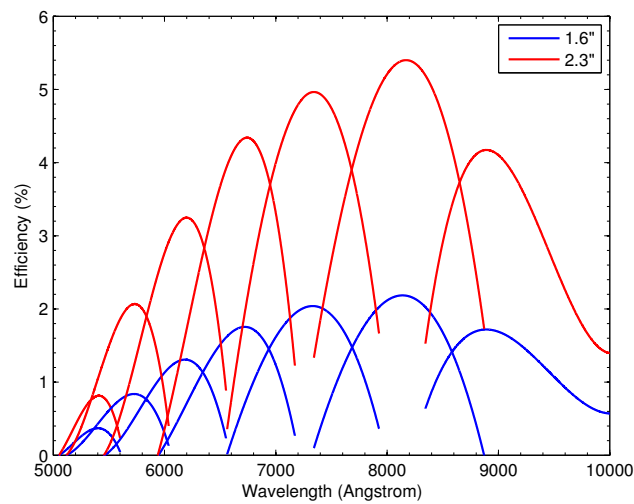


Fig. 7 The total efficiencies of E9+G12, estimated from the observations of HD 93521, with the slit widths of 1.6'' (blue lines) and 2.3'' (red lines).

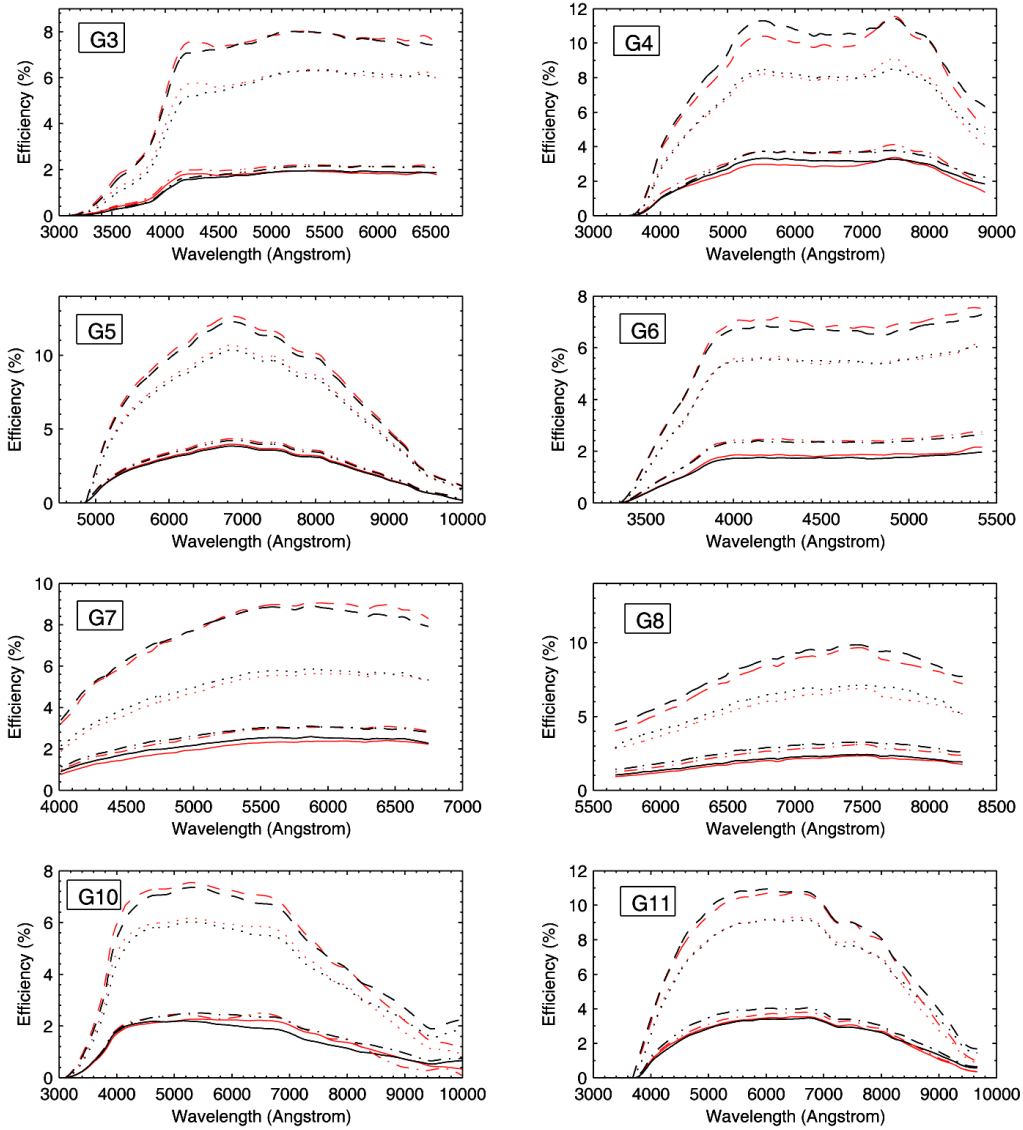


Fig. 8 The results of observing Feige 34 (red) and HD 93521 (black) with gratings G3/G4/G5/G6/G7/G8/G10/G11 and slit widths of 1.8'' (solid), 2.3'' (dash-dotted), 7.0'' (dotted) and 14.0'' (dashed).

34 and HD 93521 with the slit widths of 1.8'', 2.3'', 7.0'' and 14.0''. As shown in Figure 8, we can clearly find a difference in the total efficiencies when choosing different slit widths. For the same grism, the total efficiencies rise with increasing slit widths. However, we do not find a clear relationship between different brightnesses of stars and efficiency estimations in this work.

4.3 Impact of Weather Conditions on the Efficiency Estimations

We investigate the influence of weather conditions (seeing) on the efficiency estimations of the telescope with

BFOSC. In this work, we use the full width at half maximum (FWHM) of the star imaging profile, obtained by Gaussian fitting, to estimate the influence of seeing. Figure 9 shows the relationship between the percentage of energy of a star within the slit and different seeings. At XO, the mean seeing value is 1.9'' (Zhang et al. 2015), therefore, when we do the simulation, the seeing we adopt is 2.0''. We numerically simulate the Gaussian FWHM with slit widths of 1.8'' and 2.3'', and obtain the energy within the slit widths: 73.70% for 1.8'' and 82.64% for 2.3''. With the same method, for the seeing of 3.0'', we obtain the energy within the slit widths: 54.43% for 1.8'' and 63.35% for 2.3''. As displayed in Figure 9,

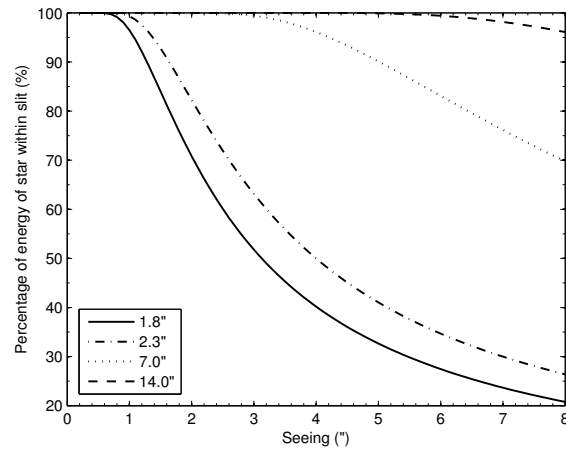


Fig. 9 The relationship between the percentage of energy of a star within the slit and different seeings. The *solid line*, *dash-dotted line*, *dotted line* and *dashed line* represent the slit widths of 1.8'', 2.3'', 7.0'' and 14.0'', respectively.

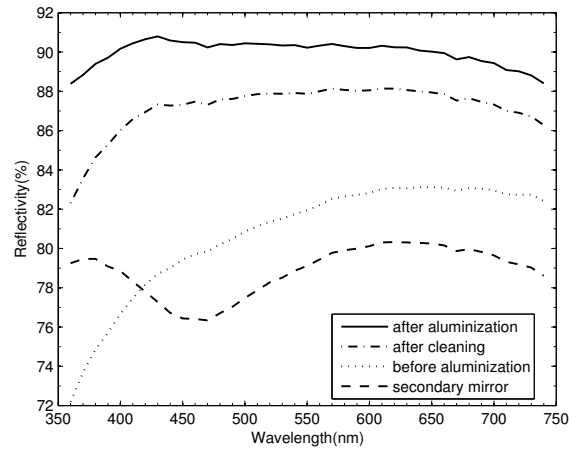


Fig. 10 The reflectivity curves of the primary and secondary mirrors of the 2.16-m reflector. The *solid line*, *dash-dotted line* and *dotted line* are the reflectivity curves obtained after aluminization, after cleaning (before aluminization) and before aluminization of the 2.16-m primary mirror, respectively. The *dashed line* is the reflectivity curve of the secondary mirror.

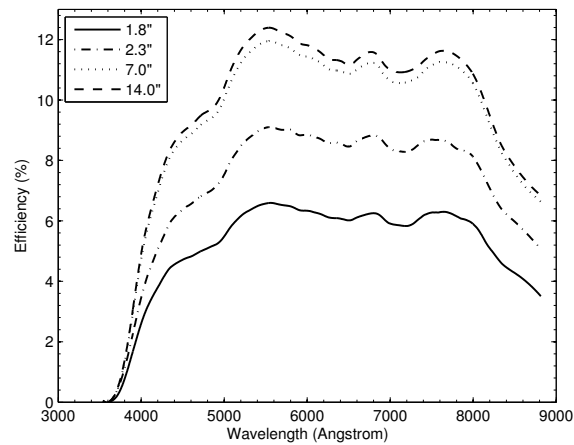


Fig. 11 The total efficiencies of grism G4 with different slit widths, after aluminization of the primary mirror of the 2.16-m reflector. The linetypes of *solid*, *dash-dotted*, *dotted* and *dashed* represent the slit widths of 1.8'', 2.3'', 7.0'' and 14.0'', respectively.

we can clearly find the seeing significantly affects the percentage of energy of a star within the slit, especially for slit widths of $1.8''$ and $2.3''$. Thus, the weather conditions also influence the efficiency of the telescope and spectrograph, depending on the slit width chosen during observations.

4.4 Impact of Mirror Reflectivities on the Efficiency Estimations

It is easy to understand that the reflectivities of the primary and secondary mirrors play an important role in the total efficiency of the telescope with BFOSC. The primary mirror of the 2.16-m reflector is usually aluminized in August or September every year.

In 2017, time that the primary mirror was aluminized was during the period September 4th–11th. We used a CM-2600d⁵ spectrophotometer to measure the reflectivities of the primary and secondary mirrors, the results of which are shown in Figure 10. The solid line, dash-dotted line and dotted line represent the reflectivity curves after aluminization, after cleaning (before aluminization) and before aluminization of the 2.16-m primary mirror, respectively. The dashed line is the reflectivity curve of the secondary mirror. As displayed in Figure 10, we can see that the reflectivity of the primary mirror decreases from $\sim 5.99\%$ (in $\sim 7400 \text{ \AA}$) to $\sim 16.00\%$ (in $\sim 3600 \text{ \AA}$) in one year. However, after cleaning the primary mirror, the reflectivity usually improved in the whole wavelength coverage. Since the secondary mirror has been used for ten years, we plan to aluminize it in the next work.

After aluminization of the primary mirror, we measured the total efficiency of the telescope with BFOSC following the method mentioned above. Since the two standard stars HD 93521 and Feige 34 were not observable at this time, we chose another standard star HR8634 ($V = 3.40$ mag, spectral type B8V) from the ESO website. HR8634 was observed with the grism G4 with slit widths of $1.8''$, $2.3''$, $7.0''$ and $14.0''$ on 2017 September 16, which are illustrated in Figure 11 with solid, dot-dashed, dotted and dashed lines respectively. The seeing was $\sim 2.0''$ during the observations. Compared with Figure 8 (the grism G4), we can see the peaks of total efficiencies have been improved to $\sim 3.1\%$, $\sim 5.0\%$, $\sim 2.9\%$ and $\sim 0.8\%$ with the slit widths of $1.8''$, $2.3''$, $7.0''$ and $14.0''$, respectively. It can also be noted that

in the blue-band ($\sim 5549 \text{ \AA}$), the total efficiencies have been improved to $\sim 3.6\%$, $\sim 5.4\%$, $\sim 3.7\%$ and $\sim 2.0\%$ with the slit widths of $1.8''$, $2.3''$, $7.0''$ and $14.0''$, respectively. While in the red-band ($\sim 7656 \text{ \AA}$), the improvements are $\sim 2.9\%$, $\sim 4.9\%$, $\sim 2.0\%$ and $\sim 0.5\%$ with the slit widths of $1.8''$, $2.3''$, $7.0''$ and $14.0''$, respectively. These cases demonstrate that aluminization is more important for the improvement of total efficiency in the blue-band ($\sim 5549 \text{ \AA}$) than in the red-band ($\sim 7656 \text{ \AA}$). As the seeing was $\sim 2.0''$ during the observations of HR8634, which was better than during the observations of the HD 93521 and Feige 34 ($\sim 3.0''$), combined with Figure 9, this demonstrates the seeing significantly affects the total efficiency of the telescope with BFOSC, especially for the slit widths of $1.8''$ and $2.3''$.

5 CONCLUSIONS

We systematically investigated the total efficiency (including atmospheric extinction, reflectivity of the primary and secondary mirrors, transmissions of gratings and quantum efficiency of the CCD) of different gratings used in the BFOSC with different slit widths, and analyzed the factors that possibly impact the efficiency of the telescope and spectrograph, which are important for observations and operations of the telescope. The grism G12 has the highest peak total efficiency ($\sim 13.0\%$) among all the gratings used in BFOSC at the wavelength of $\sim 6876 \text{ \AA}$. For echelles, E9+G12 has the highest peak of total efficiency ($\sim 5.4\%$ at the wavelength of $\sim 8160 \text{ \AA}$). For wavelength range of $3300 - 7000 \text{ \AA}$, the total efficiency of grism G7 is the highest ($\sim 8.9\%$ at the wavelength of $\sim 5861 \text{ \AA}$); for the wavelength range of $5200 - 10000 \text{ \AA}$, the total efficiency of grism G12 is the highest ($\sim 13.0\%$ at the wavelength of $\sim 6876 \text{ \AA}$); for wavelength range of $3600 - 8700 \text{ \AA}$, the total efficiency of grism G4 is the highest (~ 11.5 at the wavelength of $\sim 5371 \text{ \AA}$). As the median and mean seeing values of XO are around $1.7''$ and $1.9''$, respectively (Zhang et al. 2015), we recommend observers to use the slit width of $1.8''$ or $2.3''$.

After investigating the reflectivities of the primary and secondary mirrors of the 2.16-m reflector, we suggest that the mirrors should be cleaned and aluminized annually, especially after the pollen season and dust storms in spring, at least once per year. Comparing the total efficiencies obtained before and after aluminization of the primary mirror of the 2.16-m reflector, we can see in the blue-band ($\sim 5549 \text{ \AA}$), the total efficiencies have

⁵ <https://sensing.konicaminolta.us/products/cm-2600d-spectrophotometer/>

been improved $\sim 3.6\%$, $\sim 5.4\%$, $\sim 3.7\%$ and $\sim 2.0\%$ with slit widths of $1.8''$, $2.3''$, $7.0''$ and $14.0''$, respectively. While in the red-band ($\sim 7656 \text{ \AA}$), the improvements are $\sim 2.9\%$, $\sim 4.9\%$, $\sim 2.0\%$ and $\sim 0.5\%$ with slit widths of $1.8''$, $2.3''$, $7.0''$ and $14.0''$, respectively. These results demonstrate that aluminization is more important for the improvement of total efficiency in the blue-band than in the red-band. The seeing also significantly affects the total efficiency of the telescope with BFOSC, especially for slit widths of $1.8''$ and $2.3''$.

From the total efficiencies of the 2.16-m telescope and BFOSC, we can see that the peak of the total efficiencies (including atmospheric extinction, reflectivity of the primary and secondary mirrors, transmissions of the grisms and quantum efficiency of the CCD) of the 2.16-m reflector and BFOSC are around 6.6%–13.0%. We will carry out more detailed investigations and improve the efficiency of the telescope and instrument in future work.

Acknowledgements This work is supported by the Open Project Program of the Key Laboratory of Optical Astronomy, National Astronomical Observatories, Chinese Academy of Sciences, and the National Natural

Science Foundation of China (Grant Nos. 11503045 and 11373003), National Program on Key Research and Development Project (2016YFA0400804) and National Key Basic Research Program of China (2015CB857002). We acknowledge support from the staff of the Xinglong 2.16-m telescope, and thank Dr. Meng Zhai and night assistants of the 2.16-m telescope for their kind support with obtaining data.

References

- Fan, Z., Wang, H., Jiang, X., et al. 2016, *PASP*, 128, 115005
- Huang, L., Wu, H., Li, H.-B. 2012, “BFOSC (Beijing Faint Object Spectrograph and Camera) Operating Manual”, http://www.xinglong-naoc.org/attached/File/20150426/BFOSCmanualv2.2_chinese.doc
- Sheinis, A., Anguiano, B., Asplund, M., et al. 2015, *Journal of Astronomical Telescopes, Instruments, and Systems*, 1, 035002
- Su, D.-Q., Zhou, B.-F., & Yu, X.-M. 1989, *Science In China (A)*, 11, 1187
- Wampler, E. J., & Morton, D. C. 1977, *Vistas in Astronomy*, 21, 191
- Zhang, J.-C., Ge, L., Lu, X.-M., et al. 2015, *PASP*, 127, 1292